JOURNAL OF SOLID STATE CHEMISTRY **126,** 300–307 (1996)
ARTICLE NO. 0341

New High-Pressure Phase and Pressure-Induced Amorphization of $Ca(OH)_2$: Grain Size Effect

S. Ekbundit, K. Leinenweber, J. L. Yarger, J. S. Robinson, M. Verhelst-Voorhees, and G. H. Wolf

Department of Chemistry and Biochemistry, Arizona State University, Tempe, Arizona 85287-1604

Received March 18, 1996; in revised form June 6, 1996; accepted July 2, 1996

In situ **high-pressure Raman spectroscopy was used to investigate the phase stability of powder and single crystal portlandite, $Ca(OH)_2$, up to 22 GPa. Our results show that the room temperature, high-pressure behavior of this compound is strongly influenced by grain size. Compression of fine grained powder $Ca(OH)_2$ (<500 Å in thickness) leads to pressure-induced amorphization at around 11 GPa, as shown by extreme broadening of the Raman features. This is in agreement with previous studies of powder samples of $Ca(OH)_2$. However, when single crystal samples (thickness ~10 μm) are used, new Raman peaks replace the portlandite spectrum at 6 GPa, indicating a crystal-to-crystal phase transformation. The new Raman spectrum does not match either of the two known phases, portlandite or the baddeleyite form. A comparative Raman study shows that the new phase resembles $Sr(OH)_2$. The new form of $Ca(OH)_2$ eventually undergoes pressure-induced amorphization around 20 GPa, suggesting that it is not thermodynamically stable at this condition. Under decompression, both single crystal and fine grained samples completely revert back to portlandite. These observations suggest that small grain size can stabilize the low-pressure phase in the powder samples, thus allowing the 6 GPa phase transformation to be by-passed and amorphization to occur.**

INTRODUCTION

Interest in spectroscopy of portlandite, $Ca(OH)_2$, began in the early twentieth century when its complex IR spectrum was observed and seemed to be in conflict with the crystal structure elucidated from X-ray diffraction. After further investigation, the structure of portlandite was confirmed to be in the hexagonal system with space group $P\bar{3}m1$ (D_{3d}^3), based on both X-ray (1, 2) and neutron diffraction data (3), and the infrared data were reinterpreted to be consistent with this determination (4). $Ca(OH)_2$ is a layered compound (Fig. 1) and may be considered as a quasi-two-dimensional crystal. Many divalent hydroxides such as $Mg(OH)_2$, $Ni(OH)_2$, and $Co(OH)_2$ also crystallize in this structure. In these compounds, the hydrogen atoms exhibit a large degree of thermal motion in the plane perpendicular to the hexagonal axis (3, 5–7). Busing and Levy (3) proposed an "umbrella" shaped distribution as a model for the hydrogen motion in $Ca(OH)_2$ with the H tilted slightly off the axis parallel to the hexagonal axis. Later in 1993, Desgranges *et al.* (7) reinvestigated the structure of $Ca(OH)_2$ via neutron diffraction and proposed a three-site split-atom model for the H atom motion. In this model, hydrogens are not freely precessing around the z axis, but are localized at three equivalent sites, directed toward three oxygens in an adjacent layer (see Fig. 1). This configuration apparently favors hydrogen bond formation and, in the case of $Mg(OH)_2$, is enhanced with increasing pressure (8).

Several high-pressure X-ray studies on brucite, $Mg(OH)_2$, showed that this phase (at least the Mg–O network of the structure) persists up to 35 GPa at room temperature (9, 10). Shock experiments (11, 12) also confirmed the stability of $Mg(OH)_2$ up to 97 GPa. In contrast, $Ca(OH)_2$, $Ni(OH)_2$, and $Co(OH)_2$ all exhibit a reversible pressure-induced amorphization near 11 GPa. For $Ca(OH)_2$, this crystal-to-amorphous transition has been confirmed by X-ray diffraction (13, 14), infrared, and Raman studies (13, 15, 16), and $Ni(OH)_2$ and $Co(OH)_2$ has been inferred from *in situ* IR measurements (17, 18). The anomalous stability of crystalline $Mg(OH)_2$ in comparison to the other three isomorphic hydroxide compounds is not well understood. Duffy *et al.* (16) proposed that the disordering of the hydrogen sublattice may play an important role in amorphization of $Ca(OH)_2$, and results from the kinetic frustration of an underlying crystalline phase transformation. Recently, a pressure-induced crystalline phase transformation has been observed in $Ca(OH)_2$ at high temperature, to a baddeleyite-type (monoclinic ZrO_2) structure (19), near 9 GPa. In this high-pressure phase, the calcium atoms are in quasi-sevenfold coordination. The hydrogen positions of the baddeleyite-type $Ca(OH)_2$ phase have now been determined from powder neutron diffraction data (20).

The initial purpose of this study was to investigate the

0022-4596/96 $18.00

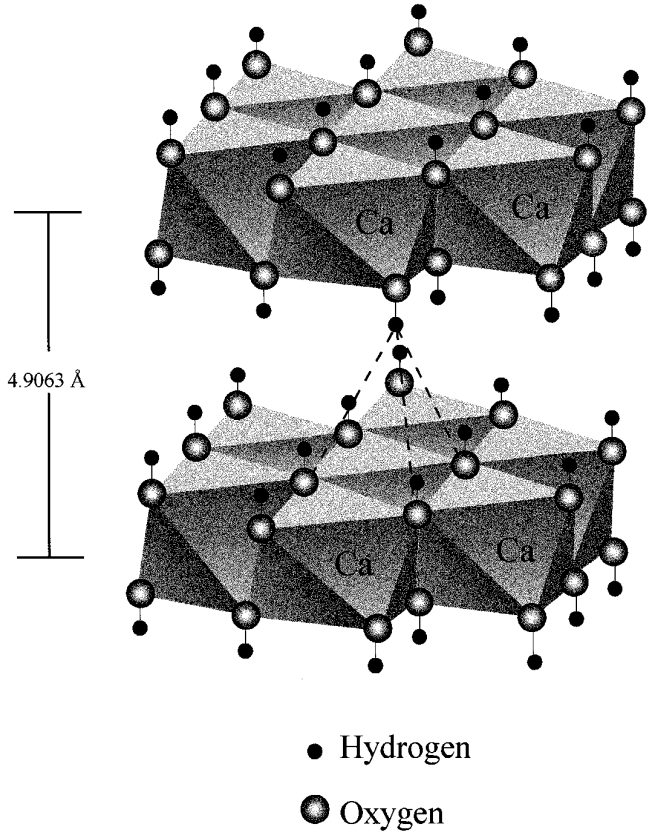

FIG. 1. Crystal structure of $Ca(OH)_2$ at ambient conditions. The dotted lines show the preferential orientations for the H atoms as described in the three-site split-atom model (see text).

hydrogen behavior of this high-pressure high-temperature phase of $Ca(OH)_2$ using Raman spectroscopy. However, in the process of synthesizing this phase for spectroscopy in the diamond anvil cell, we found a surprising result when samples of different grain sizes were used. Fine grained $Ca(OH)_2$ (thickness ~500 Å) exhibits pressure-induced amorphization near 11 GPa as previously reported. Single crystals of $Ca(OH)_2$ (thickness ~10 μm), however, undergo a reversible pressure-induced crystal-to-crystal transition near 6 GPa. This high-pressure phase in turn amorphizes near 20 GPa. The Raman spectra of this new high-pressure crystalline phase is not consistent with either the portlandite or the baddeleyite form, but closely resembles that of $Sr(OH)_2$.

In this study, the new results on single crystals are presented and compared to the present and previous results for powder samples. The grain size effect on the crystal-to-crystal phase transition and amorphization in $Ca(OH)_2$ are discussed in analogy to other systems where grain size plays a role in high-pressure phase transitions. In addition, a possible crystal structure of the high-pressure phase of the single crystal samples is proposed.

EXPERIMENTS

$Ca(OH)_2$ powder was obtained commercially from Alfa. X-ray diffraction patterns showed a trace amount (~0.5%) of $CaCO_3$ contamination. The powder sample was used with no further purification. Single crystals of $Ca(OH)_2$ were obtained by melting and recrystallizing the powder sample in the piston cylinder apparatus. The sample was brought up to 850°C and 12 kbar, above the melting curve reported by Irving *et al.* (21), and was slowly cooled isobarically to room temperature. After pressure was released, single crystals of $Ca(OH)_2$ were obtained. The average dimensions of the crystals used in this study were 50 μm × 50 μm × 10 μm, while the grain size of the powder sample was determined to be 1 μm × 1μm × 500 Å, using a combination of electron imaging with a JEOL JXA-8600 electron microprobe and analysis of the anisotropic broadening of the X-ray peaks. Both powder and single crystal samples were subjected to two conditions: nonhydrostatic (no pressure medium) and quasi-hydrostatic (argon pressure medium) environments. The samples were contained in stainless-steel gaskets drilled to 100 μm

in diameter and preindented to approximately 70–80 μm thick. Several runs were performed, using both Marrill-Bassett and Mao-Bell type diamond anvil cells, and pressure was determined by the shift in the $R1$ ruby fluorescence line (22). *In situ* Raman measurements were performed using a S.A. triple spectrometer (S3000) with a Princeton Instrument charged-coupled device (CCD) PI-1100 detector. The samples were excited with an Ar^+ Coherent 90-5 laser operating at 488 nm, and the data were collected in 180° backscattering geometry.

RESULTS

An ambient pressure Raman spectrum of $Ca(OH)_2$ is shown in Fig. 2 and is in good agreement with previous measurements. According to factor group analysis (23), there are four Raman active modes ($2A_{1g} + 2E_g$) and four infrared active modes ($2A_{2u} + 2E_u$) for this crystal structure. Since the calcium atoms are located on inversion sites, the atomic displacements associated with the Raman modes are restricted to the hydroxide sublattice. The high-frequency A_{1g} band represents the internal stretching vibration of the OH unit and occurs at 3617 cm^{-1} under ambient pressure. The remaining Raman active modes occur below 700 cm^{-1} and are considered lattice modes. The A_{1g} and E_g modes at 357 and 254 cm^{-1}, respectively, involve translational displacement of the OH unit while the E_g mode at 675 cm^{-1} involves OH rocking motion.

a. Powder Sample Spectra

The highest pressure obtained for nonhydrostatic (NH) and quasi-hydrostatic (QH) powder studies are 12.6 and 12.1 GPa, respectively. Raman spectra for the NH run are shown in Fig. 3 and are similar to those obtained for the powder sample under quasi-hydrostatic compression. Increasing pressure causes the lattice modes to shift to higher frequencies. The OH frequency, on the other hand, is red shifted upon compression, indicating an increase in the hydrogen bond strength between layers. For both NH and QH runs, all of the Raman bands broaden with increasing pressure. Near 8 GPa, there is a marked reduction in intensity and no peaks can be clearly identified above 11 GPa, denoting the onset of amorphization in powder samples. The pressure at which these samples transform to the amorphous state is in good agreement with previous studies (10, 13–15). Under decompression, the Raman bands associated with the crystalline phase are recovered below 7

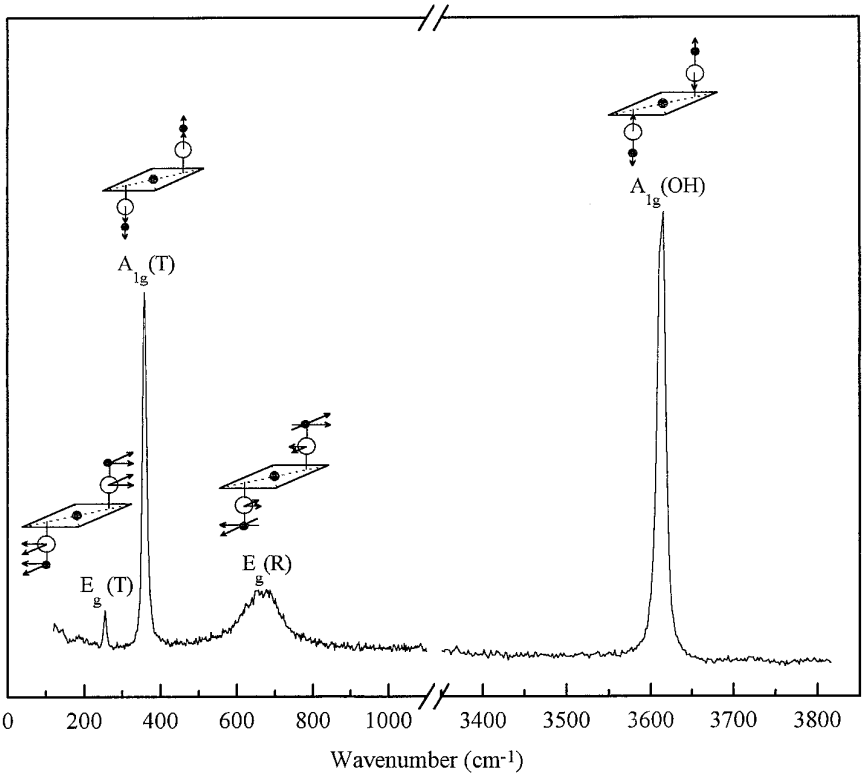

FIG. 2. Ambient Raman spectrum of $Ca(OH)_2$, along with diagrams describing atomic motions of corresponding vibrational modes. The three lattice modes occur below 700 cm^{-1}, and are located at 254 cm^{-1} ($E_g(T)$), 357 cm^{-1} ($A_{1g}(T)$), and 675 cm^{-1} ($E_g(R)$). The internal stretching frequency (A_{1g}), involving the hydroxyl stretching vibration, is located at 3617 cm^{-1}.

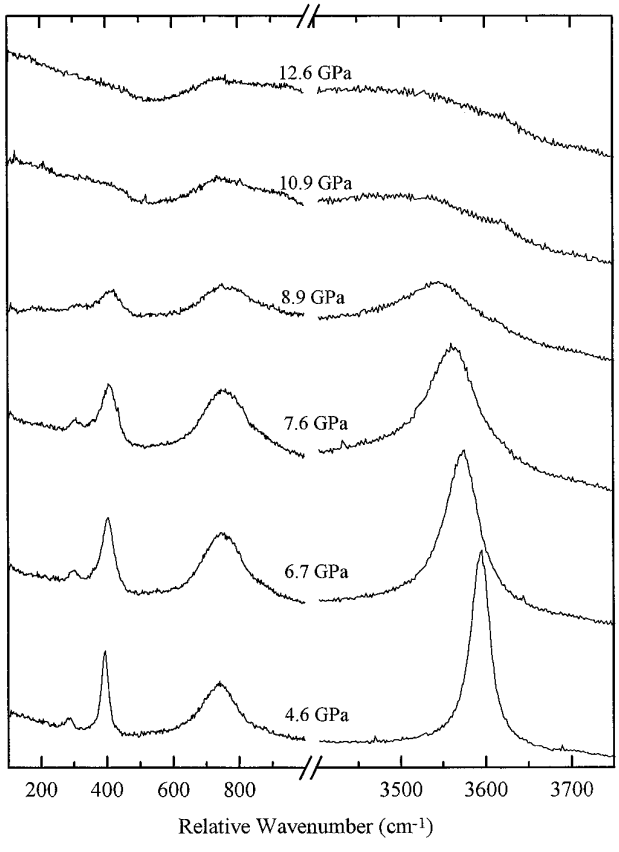

FIG. 3. Raman spectra of $Ca(OH)_2$ powder compressed nonhydrostatically. The Raman bands broaden and the intensity decreases with pressure. This sample eventually amorphizes near 11 GPa as indicated by the disappearance of the Raman bands.

GPa in the quasi-hydrostatic experiment and near 2 GPa in the nonhydrostatic experiment. No significant residual frequency shifts or broadening are observed in the Raman bands of the pressure-cycled sample compared to those of the starting material.

b. Single Crystal Spectra

The high-pressure behavior observed for the single crystal sample of $Ca(OH)_2$ is in sharp contrast to that observed in the powdered material. In quasi-hydrostatic experiments, abrupt changes in the Raman spectra are observed at about 6 GPa (see Fig. 4). The characteristic Raman bands of the portlandite phase are replaced by a number of new peaks in both the low- and high-frequency regions. These new peaks are relatively sharp, with bandwidths comparable to those of the original portlandite phase below the transition pressure, and thus indicate a crystalline phase transition. Two Raman bands are observed in the hydroxyl region above the transition pressure. One of the bands is very sharp and located at 3640 cm^{-1}; this band displays almost no change in the frequency with increasing pressure. The other band, located near 3510 cm^{-1} at 6.5 GPa, broadens significantly and exhibits a gradual reduction in frequency with pressure. All of the Raman bands of the high-pressure phase broaden and decrease in intensity with further compression. At the peak pressure of 16.5 GPa, the lattice modes are barely detectable, but the OH-stretching modes are still apparent along with a broad underlying background. Under decompression, this sample readily reverts back to portlandite with only a slight hysteresis of 1 GPa.

To confirm that this transition is not mainly driven by the presence of a soft pressure medium, additional experiments were performed using single crystal samples without

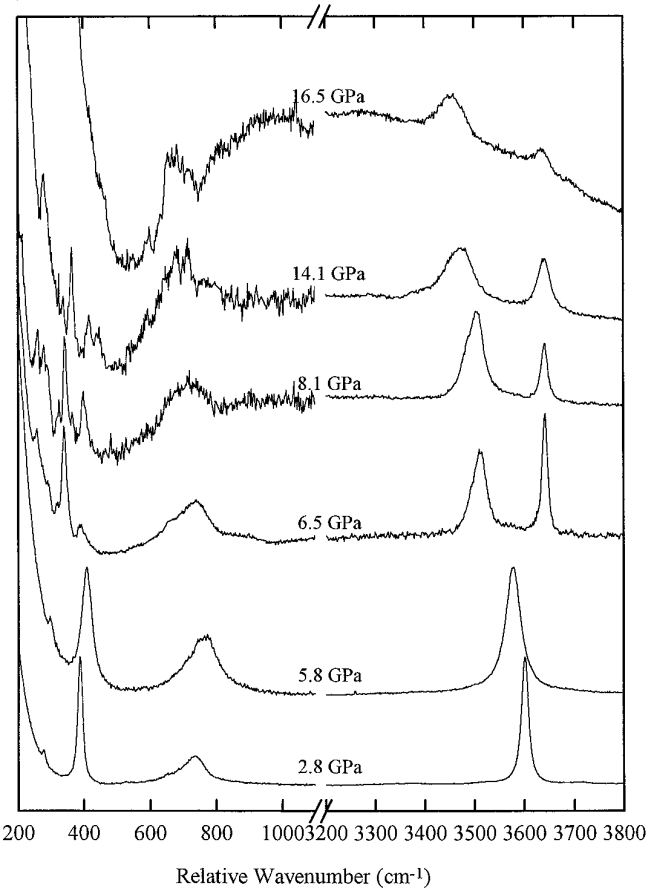

FIG. 4. Pressure-dependence of the Raman vibrations of single crystal $Ca(OH)_2$ in an argon pressure medium. Dramatic changes in the Raman spectrum are observed between 5.8 and 6.5 GPa, where the characteristic Raman bands of the portlandite phase are replaced by a number of new peaks in both low- and high-frequency regions. At the peak pressure of 16.5 GPa, the intensity of the lattice modes are very weak. The hydroxyl bands are still visible, and a broad background feature has appeared.

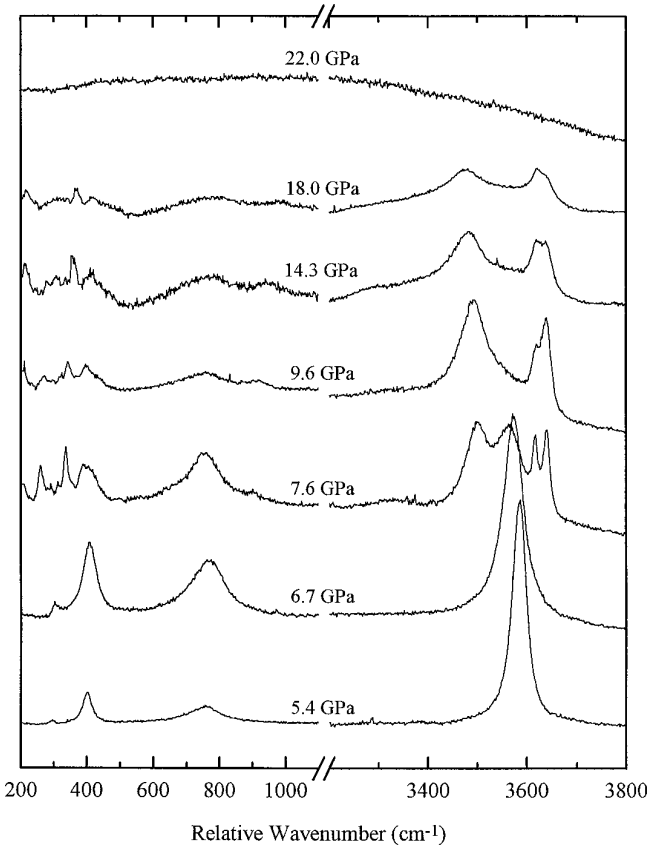

FIG. 5. Raman spectra of single crystal $Ca(OH)_2$ samples under nonhydrostatic conditions. The transformation is observed between 6.7 and 7.6 GPa. Most of the Raman frequencies of this high-pressure phase correlate well with those in the QH sample. However, more bands are observed in the hydroxyl frequency region. Further compression of this sample leads to amorphization near 22 GPa, as shown by a complete disappearance of all the crystalline Raman bands.

pressure medium. Here, a crystalline phase transition is also observed but at a slightly higher pressure (near 8 GPa), with some modification in the spectra in comparison to those of the high-pressure phase seen in the quasi-hydrostatic experiment (Fig. 5). Some of the lattice modes correlate well with those observed for the high-pressure phase in the single crystal QH run. In the hydroxyl stretching region, two extra bands are observed, in addition to the two which appear in the quasi-hydrostatic samples. These two extra modes eventually merge into the other two bands with further compression. The Raman bands become less intense as the pressure increases, and the Raman spectrum becomes featureless by 22 GPa. Upon decompression, the sample returns to the original portlandite phase between 4 and 3 GPa. In all experiments, the spectra of the quenched samples are similar to those of the uncompressed samples, indicating that all of the high-pressure behavior observed is unquenchable.

DISCUSSION

a. Comparison between Single Crystal and Powder Samples

To examine the different behaviors between powdered and single crystal samples, plots of pressure-dependence of the Raman modes are shown in Figs. 6 (lattice modes) and 7 (hydroxyl vibrations). Below 6 GPa, both powder and single crystal samples behave similarly. Above 6 GPa, the Raman bands belonging to the powdered samples continue along their original trend, and finally terminate at the crystal-to-amorphous transition pressure of 11 GPa. Single crystal samples, on the other hand, display an abrupt change in the number of modes. This behavior can be clearly identified as a crystalline transformation. Although the number of bands appearing in the NH single crystal samples is different from that observed in the QH single crystal samples, it is highly possible that the high-pressure phase obtained in the nonhydrostatic runs has a slight structural modification from the phase observed in QH single crystal samples. We will consider the spectrum taken under QH conditions to be more characteristic of the high-pressure phase of $Ca(OH)_2$ and will use it in the analysis of the phase transition.

In the hydroxyl stretching vibrations, the lowest and

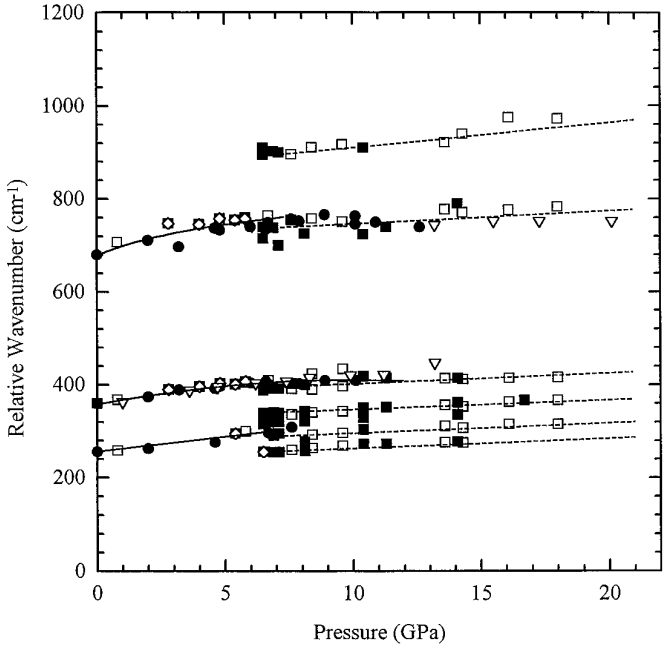

FIG. 6. Pressure-dependence of the lattice modes in all samples of $Ca(OH)_2$ up to 18 GPa. The squares represent single crystal experiments (solid, quasi-hydrostatic; open, nonhydrostatic) and the circles represent data from powder samples. Results from this study are compared to Meade *et al.* (13) (down triangles) and Duffy *et al.* (10) (diamonds), where good correspondence is achieved among the data.

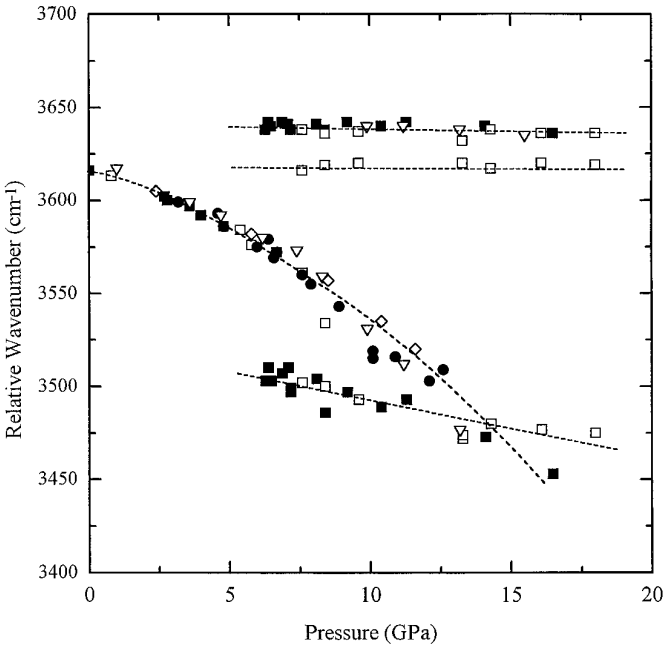

FIG. 7. Pressure-dependence of the hydroxyl stretching frequencies up to 18 GPa. The symbols are the same as in Fig. 6. The original OH vibration in portlandite decreases very rapidly with pressure. One of the modes seen in single crystal (NH) is following the trend of the powder sample, suggesting a coexistence of the amorphous material with the high-pressure phase in the nonhydrostatic sample.

highest frequencies in the NH samples correlate well with the frequencies detected in single crystal QH samples. The second lowest frequency follows the same trend of the powder sample, thus suggests the coexistence of mixed phases in the NH experiment. Finally, there is a sharp peak located at 3616 cm^{-1} in NH runs, which is not observed in the other samples. The origin of this peak is not known.

It is interesting at this point to compare this result to previous measurements. Meade *et al.* (13) reported an observation of an additional peak above 12 GPa located at 750 cm^{-1}, while no other studies have reported this feature. Apparently, this peak corresponds to a mode of the high-pressure phase seen in the present study. In addition, the hydroxyl band at 3640 cm^{-1} observed in Meade's study also coincides with one of the high-pressure phase modes found here (see Figs. 6 and 7).

b. Grain Size Effect and Amorphization

The results presented here clearly show that the high-pressure phase stability of $Ca(OH)_2$ is greatly affected by the domain size of the sample. For larger crystalline domains, on the order of tens or hundreds of micrometers, portlandite undergoes a crystal-to-crystal transformation, followed by amorphization at ~20 GPa. For much smaller grain sizes, on the order of hundreds of Angstroms in thickness, portlandite persists metastably beyond this transformation, and amorphizes at ~11 GPa. Both behaviors are reversible with a much larger hysteresis in nonhydrostatic experiments than in quasi-hydrostatic experiments.

The metastable persistence of the fine-grained portlandite is similar to previous observations for the wurtzite-to-rocksalt transition of CdSe (24) and the monoclinic-to-orthorhombic transformation in ZrO_2 (25). In these systems, the transition pressure increases as the crystallite size decreases. The ability to extend the low-pressure phase past an equilibrium phase transformation by decreasing the crystallite size is also seen in AlAs/GaAs superlattices (26). In the present example, the small grain size extends the stability of the portlandite phase far enough that the crystal-to-crystal transformation is completely suppressed, and an amorphization process takes place instead.

The simplest thermodynamic scheme which gives consistent interpretation of the energetics of this system is shown in Fig. 8. The effect of reducing the grain size causes a slight increase in the free energy of the portlandite phase. This effect must be much more significant in the high-pressure phase of $Ca(OH)_2$ such that the amorphous state becomes more stable at higher pressure; thus, the crystal-to-crystal transformation in powder sample is by-passed. For samples of larger grains (bulk sample), the free energy

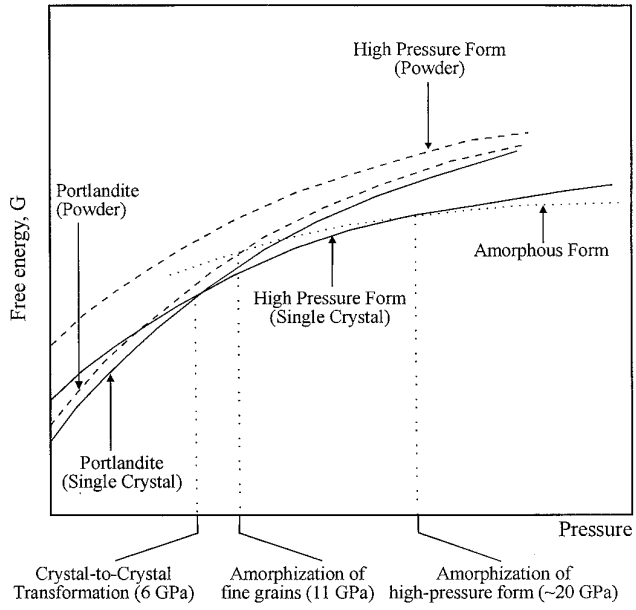

FIG. 8. Hypothetical free energy vs pressure diagram for $Ca(OH)_2$ at room temperature. The curves belonging to single crystal $Ca(OH)_2$ are shown with solid lines, while those of the powder samples are shown with dashed lines. The amorphous form is indicated by a dotted line. The crystal-to-crystal transition of single crystal samples and the amorphization of powdered samples occur at the pressures where the free energy curves of the two corresponding phases cross.

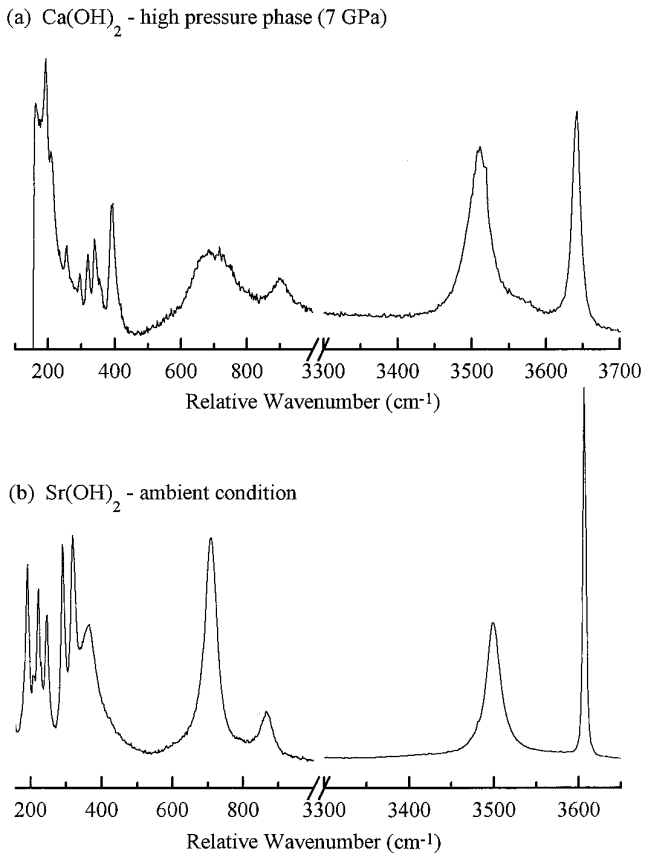

FIG. 9. Raman spectra of (a) the high-pressure form of $Ca(OH)_2$ at 7 GPa and (b) an ambient spectrum of $Sr(OH)_2$.

of the high-pressure phase intersects that of the portlandite phase around 6 GPa, and a crystal-to-crystal transformation occurs. Further increase of pressure eventually leads to the crossing of this free energy curve with that of the amorphous material, therefore the amorphization of the high-pressure phase is observed. The fact that both the high-pressure form (single crystal samples) and the portlandite phase amorphize indicate that there should exist a more stable form of $Ca(OH)_2$ with much lower energy than both the amorphous and the high-pressure forms observed here. Baddeleyite is one good candidate for a such phase.

The underlying reasons for the difference in behavior between different grain sizes of portlandite, $Ca(OH)_2$, is not clear at present. Other factors such as grain–grain contact (interfaces), high surface area, variation of composition at surfaces, structural defects, and surface contamination (i.e., $CaCO_3$) can also contribute to the high-pressure behavior of this system.

c. Identification of the High-Pressure Form

A few properties of the high-pressure phases (QH and NH) can be deduced from the resulting Raman spectra. The increasing number of the Raman bands is a good indication of the lowering of the crystal symmetry of the high-pressure phase in comparison to the portlandite phase. Also, the observed hydroxyl stretching modes indicate that there are at least two different environments for the hydrogens in the unit cell. A characteristic large bandwidth and negative shift with pressure of one of the hydroxyl bands manifests hydrogen bonding. In contrast, the hydrogen atom associated with the OH vibration at 3640 cm^{-1} is probably not hydrogen bonded since its vibration frequency remains rather constant with increasing pressure, and the bandwidth does not broaden as quickly.

The baddeleyite phase (19, 20) was considered as a possible candidate for the high-pressure phase found here. However, this phase was synthesized at 250°C in a heated diamond cell, and the spectrum (27) was found to be significantly different from that of the high-pressure phase observed here. In particular, the number of modes and their vibration frequencies in the hydroxyl stretching frequency are very distinct from those of the high-pressure phase observed here.

One strong candidate for the high-pressure phase is of the $Sr(OH)_2$ structure (28). It is appealing because the relatively high symmetry (orthorhombic) and the presence of two hydrogen sites with different bonding characteristics are consistent with the overall features of the Raman spectrum of the new phase. A comparison of the Raman spectrum of $Sr(OH)_2$ (27, 29) to that of the high-pressure $Ca(OH)_2$, indeed, reveals a striking similarity in the overall pattern and number of bands between the two phases (see Fig. 9). Further characterization of this new high-pressure phase would require an *in situ* X-ray measurement, which we hope to pursue in the future.

CONCLUSIONS

The high-pressure behavior of $Ca(OH)_2$ at room temperature is strongly dependent upon grain size. Fine powders undergo pressure-induced amorphization at 11 GPa, while single crystals experience a crystal-to-crystal phase transition at 6 GPa and then amorphize around 20 GPa. Both samples completely revert to portlandite during decompression. A simple free energy diagram explaining the origin of these observations is suggested, and the structure of the high-pressure phase is proposed to be that of $Sr(OH)_2$.

ACKNOWLEDGMENTS

The authors thank Professor Mike O'Keeffe for providing insight to structure determination and Cynthia Polsky for useful comments. Jim Clark provides us with SEM patterns. This work has been funded under the ASU Material Research Group Grant DMR-9121570.

REFERENCES

1. H. E. Petch and H. D. Megaw, *J. Opt. Soc. Am.* **44,** 744 (1954).
2. J. D. Bernal and H. D. McGaw, *Proc. R. Soc.* (*London*) *A* **151,** 384 (1935).
3. W. R. Busing and H. A. Levy, *J. Chem. Phys.* **26,** 563 (1957).
4. P. Dawson, C. D. Hadfield, and G. R. Wilkinson, *J. Phys. Chem. Solids* **34,** 1217 (1973).
5. F. Zigan and R. Rothbauer, *Neues. Jahrb. Mineral. Monatsh.,* 137 (1967).
6. C. Greaves and M. A. Thomas, *Acta Cyrstallogr. B* **42,** 51 (1986).
7. L. Desgranges, D. Grebille, G. Calvarin, G. Chevrier, N. Floquet, and J.-C. Niepce, *Acta Crystallogr. B* **49,** 812 (1993).
8. J. B. Parise, K. Leinenweber, D. J. Weidner, K. Tan, and R. B. Von Dreele, *Am. Mineral.* **79,** 193 (1994).
9. Y. Fei and H.-K. Mao, *J. Geophy. Res.* **98,** 11875 (1995).
10. T. S. Duffy, J. Shu, H.-K. Mao, and R. J. Hemley, *Phys. Chem. Miner.* **22,** 227 (1995).
11. T. S. Duffy and T. J. Ahrens, *J. Geophys. Res.* **96,** 14,319 (1991).
12. G. V. Simakov, M. N. Pavlovsky, N. G. Kalashnikov, and R. F. Trunin, *Izv. Earth Phys.* **10,** 11 (1974).
13. C. Meade, R. Jeanloz, and R. J. Hemley, ''High Pressure Research: Application to Earth and Planetary Science'' (Y. Syono and M. H. Manghnani, Eds.), p. 485. Terra Scientific, Tokyo, 1992.
14. C. Meade and R. Jeanloz, *Geophys. Res. Lett.* **17,** 1157 (1990).
15. M. B. Kruger, Q. William, and R. Jeanloz, *J. Chem. Phys.* **91,** 5910 (1989).
16. T. S. Duffy, R. J. Hemley, and H.-K. Mao, ''Deep Earth and Planetary Volatiles.'' AIP, New York, 1994.
17. J. H. Nguyen, M. B. Kruger, and R. Jeanloz, *Phys. Rev. B* **49,** 3734 (1994).
18. J. H. Nguyen, R. Jeanloz, and M. Kruger, AGU Fall Meeting **75,** 652 (1994).
19. M. Kunz, K. Leinenweber, J. B. Parise, T.-C. Wu, W. A. Bassett, K. Brister, D. J. Weidner, M. T. Vaughan, and Y. Wang, *High Pressure Res.* **14**(4–6), 311 (1996).
20. K. Leinenweber, D. Partin, U. Schulcke, M. O'Keefe, and Von Dreele, in preparation.
21. A. J. Irving, W. L. Huang, and P. J. Wyllie, *Am. J. Sci.* **277,** 313 (1977).
22. H.-K. Mao and P. M. Bell, *J. Geophys. Res.* **91,** 4673 (1986).
23. R. A. Buchanan, H. H. Caspers, and J. Murphy, *Appl. Opt.* **2,** 1147 (1963).
24. S. H. Tolbert and A. P. Alivisatos, *Science* **265,** 373 (1994).
25. S. Kawasaki, T. Yamanaka, S. Kume, and T. Ashida, *Solid State Commun.* **76,** 527 (1990).
26. B. A. Weinstein, L. J. Cui, U. D. Venkateswaran, and F. A. Chambers, ''Frontiers of High-Pressure Research.'' Plenum Press, New York, 1991.
27. S. Ekbundit, K. Leinenweber, and G. H. Wolf, in preparation.
28. D. E. Partin and M. O'Keeffe, *J. Solid State Chem.* **119,** 157 (1995).
29. H. D. Lutz, W. Eckers, G. Schneider, and H. Haeuseler, *Spectrochimica Acta. A* **37,** 561 (1981).